Published April 7, 2014

The BTB-ZF transcription factor Zbtb20 is driven by Irf4 to promote plasma cell differentiation and longevity

Stéphane Chevrier,[1,4] Dianne Emslie,[1,4] Wei Shi,[2,5] Tobias Kratina,[1,4] Cameron Wellard,[3,4] Alexander Karnowski,[7] Erdem Erikci,[8] Gordon K. Smyth,[2,6] Kamal Chowdhury,[8] David Tarlinton,[3,4] and Lynn M. Corcoran[1,4]

[1]Molecular Immunology Division, [2]Bioinformatics Division, [3]Immunology Division, The Walter and Eliza Hall Institute, Parkville, Victoria 3052, Australia
[4]Department of Medical Biology, [5]Department of Computing and Information Systems, [6]Department of Mathematics and Statistics, The University of Melbourne, Parkville, Victoria 3010, Australia
[7]CSL Limited, Bio21 Institute, Parkville, Victoria 3010, Australia
[8]Department of Molecular Cell Biology, Max Planck Institute of Biophysical Chemistry, 37077 Göttingen, Germany

The transcriptional network regulating antibody-secreting cell (ASC) differentiation has been extensively studied, but our current understanding is limited. The mechanisms of action of known "master" regulators are still unclear, while the participation of new factors is being revealed. Here, we identify Zbtb20, a Bcl6 homologue, as a novel regulator of late B cell development. Within the B cell lineage, Zbtb20 is specifically expressed in B1 and germinal center B cells and peaks in long-lived bone marrow (BM) ASCs. Unlike Bcl6, an inhibitor of ASC differentiation, ectopic Zbtb20 expression in primary B cells facilitates terminal B cell differentiation to ASCs. In plasma cell lines, Zbtb20 induces cell survival and blocks cell cycle progression. Immunized Zbtb20-deficient mice exhibit curtailed humoral responses and accelerated loss of antigen-specific plasma cells, specifically from the BM pool. Strikingly, Zbtb20 induction does not require Blimp1 but depends directly on Irf4, acting at a newly identified Zbtb20 promoter in ASCs. These results identify Zbtb20 as an important player in late B cell differentiation and provide new insights into this complex process.

CORRESPONDENCE
Lynn M. Corcoran:
corcoran@wehi.edu.au

Abbreviations used: ADM, adriamycin; ASC, antibody-secreting cell; BTB-ZF, broad complex, tramtrack, bric-à-brac, and zinc finger; CDK, cyclin dependent kinase; CSR, class switch recombination; ΔZF, DNA binding zinc finger domain deleted; ER, estradiol receptor; Eto, etoposide; FDR, false discovery rate; GC, germinal center; GMFI, geometric mean fluorescence intensity; NP, 4(hydroxy-3)-nitrophenyl acetyl; PerC, peritoneal cavity; PI, propidium iodide; SP, spleen; SRBC, sheep red blood cells; Tfh, T follicular helper; TSS, translational start site.

Antibody-secreting cell (ASC) differentiation usually follows two routes: the extrafollicular pathway engenders a first wave of low affinity, short-lived ASCs, usually secreting IgM (MacLennan et al., 2003; Manz et al., 2005). Subsequently, the follicular pathway involves the formation of germinal centers (GCs), where B cells, interacting with T follicular helper (Tfh) and follicular dendritic cells, undergo somatic hypermutation and class switch recombination (CSR; Victora and Nussenzweig, 2012). Within the GC, cells expressing an antigen receptor of high affinity are positively selected, and will leave the GC either as memory cells, plasmablasts, or plasma cells (Oracki et al., 2010; McHeyzer-Williams et al., 2012). Some post-GC ASCs migrate to survival niches in the BM to become long-lived, nondividing plasma cells (Oracki et al., 2010).

The transcriptional program that regulates GC and ASC differentiation is tightly regulated to enable a rapid and appropriate response. A current model of plasma cell formation posits that Pax5 maintains B cell identity through induction of genes required for B cell function and repression of genes that drive ASC differentiation (Cobaleda et al., 2007). In GCs, B cell differentiation is inhibited by Bcl6 and Bach2, two factors that block Blimp1 expression, thus enabling affinity maturation and CSR (Tunyaplin et al., 2004; Muto et al., 2010). In this context, Bcl6 also promotes cell proliferation through p21 inhibition (Phan et al., 2005). Simultaneously, Bcl6 represses the Bcl2 prosurvival factor, rendering cells more susceptible to apoptosis, thus ensuring that only cells with a high affinity for antigen can survive and further differentiate (Saito et al., 2009). Blimp1 is a master regulator, both

The Rockefeller University Press $30.00
J. Exp. Med. 2014 Vol. 211 No. 5 827-840
www.jem.org/cgi/doi/10.1084/jem.20131831

Supplemental Material can be found at:
http://jem.rupress.org/content/suppl/2014/04/03/jem.20131831.DC1.html

Published April 7, 2014

necessary and sufficient for B cells to differentiate fully into ASCs (Turner et al., 1994; Shaffer et al., 2002; Shapiro-Shelef et al., 2003). Once induced, Blimp1 represses Pax5, Bcl6, and Bach2, extinguishing the B cell phenotype and enforcing ASC differentiation. Blimp1 blocks proliferation through repressing *c-Myc* (Lin et al., 1997) and indirectly induces Xbp-1, a factor critical for the unfolded protein response that enables high-level antibody secretion (Shaffer et al., 2004; Taubenheim et al., 2012).

Irf4 expression is maintained at a low level by Mitf in mature B cells (Lin et al., 2004) and is further down-regulated in GC B cells. Nevertheless, Irf4 is required for the generation of GCs and for CSR (De Silva et al., 2012; Ochiai et al., 2013), and is essential for plasma cell development (Klein et al., 2006; Sciammas et al., 2006).

Despite these advances, it is still unclear how Irf4 controls very different transcriptional programs in pre- and post-GC cells (De Silva et al., 2012). Furthermore, as immature preplasmablasts can arise from Blimp1-deficient B cells, Blimp1 cannot be the factor that initiates the program of ASC differentiation, though it is required for its completion (Kallies et al., 2007). Conversely, induction of Blimp1 in the absence of Irf4 fails to drive plasma cell differentiation (Klein et al., 2006). Thus, the current model of the transition from B cell to ASCs is incomplete, with other factors likely to be involved (Klein and Dalla-Favera, 2007).

The present study identifies Zbtb20 as a new regulator of plasma cell differentiation. This protein, also named Zfp288, DPZF (Zhang et al., 2001), and HOF (Mitchelmore et al., 2002), is a broad complex, Tramtrack, Bric-à-brac, and Zinc Finger (BTB-ZF) protein, homologous to Bcl6. BTB-ZF proteins are an emerging group of regulators, acting mainly as repressors, in many aspects of development, cancer, and lymphoid lineage differentiation (Kelly and Daniel, 2006; Costoya, 2007; Beaulieu and Sant'Angelo, 2011).

Zbtb20 was originally identified in human dendritic cells (Zhang et al., 2001) and in the developing central nervous system (Mitchelmore et al., 2002). Two different isoforms, $Zbtb20^{S}$ and $Zbtb20^{L}$, are generated by alternative splicing and translational start sites (Mitchelmore et al., 2002), but are indistinguishable in terms of function (Nielsen et al., 2007). They can dimerize in vitro via their BTB domains, are nuclear and bind to DNA via the five *Krüppel*-type zinc finger domains (Mitchelmore et al., 2002). Zbtb20-deficient mice exhibit perinatal lethality, with early growth abnormalities (Sutherland et al., 2009; Rosenthal et al., 2012). Conditional deletion of Zbtb20 in the liver highlights its involvement in metabolism (Xie et al., 2008; Peterson et al., 2011), and in the nervous system, Zbtb20 is involved in cortex formation and neuronal specification (Nielsen et al., 2007; Rosenthal et al., 2012). To date however, no role for Zbtb20 in the adaptive immune system has been described.

Here, we show that within the B cell lineage, Zbtb20 is constitutively expressed in peritoneal B1 cells, but not expressed in follicular B cells. It is induced in GC B cells and is highest in mature plasma cells of the BM. Ectopic expression of Zbtb20 in cell lines and in primary B cells promotes the plasma cell differentiation program and impacts critical aspects of late B cell differentiation, such as cell proliferation and survival. Whereas B1 and GC cells develop normally in Zbtb20-deficient mice, Zbtb20 loss curtails antibody responses upon immunization and causes a selective disappearance of BM ASCs over time. Interestingly, Zbtb20 expression is dependent on Irf4, which binds to a newly identified Zbtb20 promoter specifically active in ASCs.

RESULTS

Identification of a new BTB-ZF gene highly expressed in plasma cells

A deep understanding of ASC biology is hampered by their rarity and by the paucity of markers available to purify them. To identify new plasma cell–specific molecules, resting B cells, and ASCs at different stages of differentiation were isolated from the spleen and BM of $Blimp1^{gfp/+}$ reporter mice (Kallies et al., 2004). Microarray analyses revealed that, like genes known to be induced in ASCs, such as *Sdc1* (syndecan-1), *Xbp1*, and *Irf4*, the transcriptional repressor Zbtb20 was strongly up-regulated during plasma cell differentiation (Fig. 1 A).

Graded expression of Zbtb20 in follicular B cell response

We performed quantitative PCR (qPCR) for Zbtb20 on sorted cells representing different stages of B cell development. *Zbtb20* mRNA was low in developing B cells, but highly expressed in peritoneal B1 cells, GC B cells, and in splenic and BM plasma cells (Fig. 1 B). Using our in-house generated monoclonal antibody in intracellular flow cytometric analysis, we could confirm that all populations expressing *Zbtb20* mRNA were positive at the protein level (Fig. 1 C). Zbtb20 expression progressively increased from B1 and GC cells, through immature $Blimp1/GFP^{lo}$ plasmablasts in the spleen to $Blimp1/GFP^{hi}$ plasma cells in the BM (Fig. 1 D). Consistent with those data, immunohistochemistry on spleen after NP-KLH immunization revealed that weak Zbtb20 staining colocalized with GC structures, whereas strong staining could be observed in individual cells (Fig. 1 E). Co-staining with an anti–syndecan-1 antibody revealed that some of these cells were also syndecan-1^{+}, and hence likely ASCs (unpublished data). These data identify Zbtb20 as a transcription factor constitutively expressed in B1 cells and induced upon antigen dependent activation of follicular B cells, culminating with highest expression in mature ASCs.

Zbtb20 expression in cell lines reflects its primary B cell profile

As the B lineage cells that normally express Zbtb20 in vivo are rare or difficult to culture, we used cell lines representing different stages of B cell development as tools to discover potential functions of Zbtb20 within the B cell lineage. Zbtb20 expression was low in the immature WEHI231 and the mature I29B cell lines, but increased in A20, a GC B cell lymphoma (with high Bcl6 and AID, low Blimp1, and Irf4 expression; Fig. 2 A). Consistent with our ex vivo data, most plasmacytomas

Published April 7, 2014

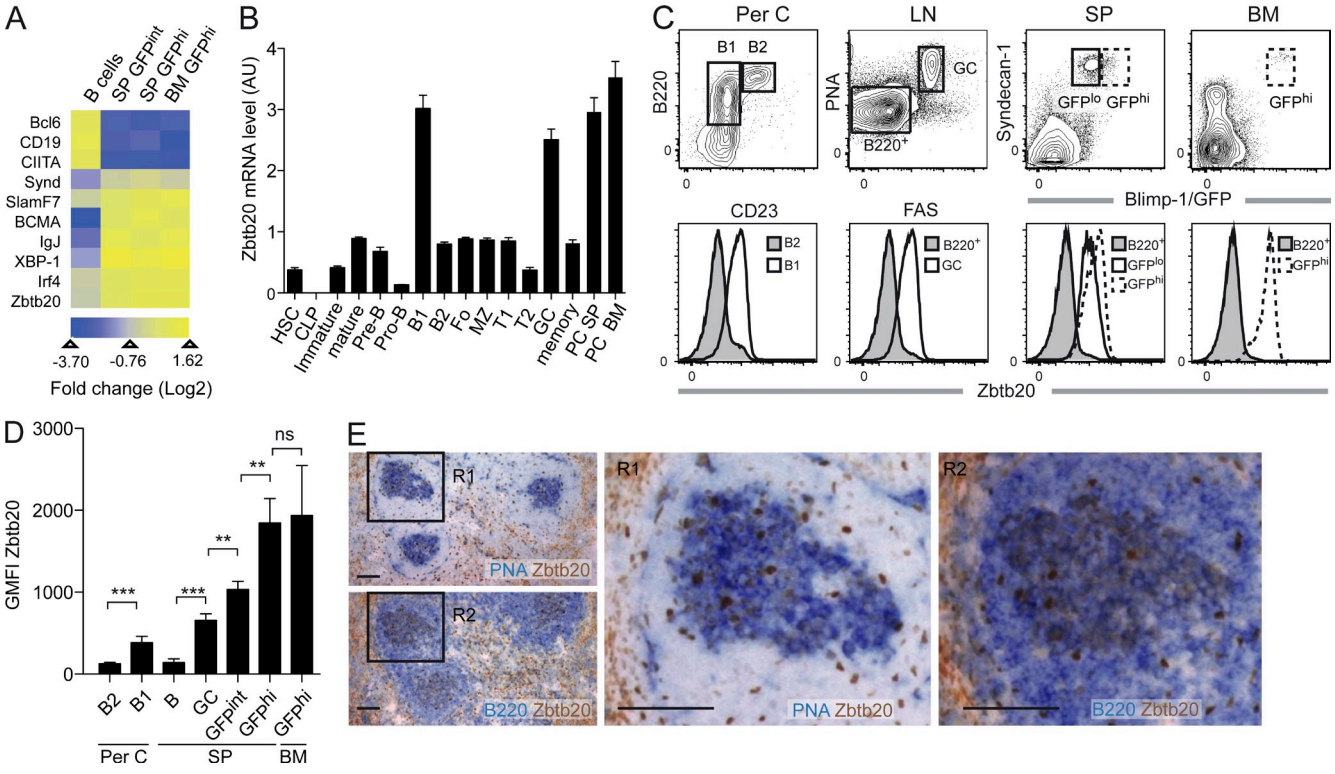

Figure 1. Zbtb20 is expressed during late B cell differentiation. (A) B cells and ASCs were isolated from the spleen and BM of *Blimp*$^{gfp/+}$ reporter mice and analyzed by microarray. Heatmap represents normalized expression of selected genes modulated during late B cell differentiation. Representative of two independent experiments. (B) qPCR to assess Zbtb20 expression in the indicated populations purified from C57BL/6 mice. Bars represent mean ± SD of triplicates. Representative of three independent experiments, using three mice in each. AU, arbitrary unit; HSC, hematopoietic stem cells; CLP, common lymphoid progenitor; Fo, follicular B cells; MZ, marginal zone B cells; T1/2, transitional 1/2 B cells. (C) Flow cytometry to identify B1 and ASC in peritoneal cavity (PerC), spleen (SP) and BM from 8–12 wk old naive mice (top). For GC, LN from SRBC immunized mice at day 10 were used. Zbtb20 expression was assessed by intracellular staining in the gated populations (bottom panels). Resting B cells were used as an internal negative control (gray histogram). Data are representative of at least six independent experiments using two mice in each. (D) Geometric mean fluorescence intensity (GMFI) of Zbtb20 in the indicated B cell populations as assessed in C. Bars are mean ± SD of three independent experiments with two mice in each. From left to right: ***, $P < 0.0001$; ***, $P < 0.0001$; **, $P = 0.0030$; **, $P = 0.0021$ (Student's *t* test). (E) Immunohistochemical analysis on spleen sections of WT mice 10 d after NP-KLH immunization. Serial sections were used to show colocalization of PNA in R1 and Zbtb20 in R2. Data are representative of three independent experiments. PNA, peanut agglutinin. Bars, 50 µm.

(J558, MPC11, and 5T33MM) displayed high Irf4 and Blimp1 expression, and expressed Zbtb20 in the nucleus. Only plasmacytoma P3 exhibited low Zbtb20 levels. All the cells that were positive for Zbtb20 expressed both isoforms equally (Fig. 2 A and not depicted). This strong correlation between Zbtb20 expression in primary B cells and their cell line counterparts suggested that the latter were appropriate models to explore Zbtb20 function during B cell differentiation.

Zbtb20 affects cell survival and cell proliferation in a plasma cell line

A retroviral vector was designed to overexpress Zbtb20 in an inducible manner (Fig. 2 B). Sequences encoding Zbtb20 and the human estradiol receptor (ER) dimerization domain were fused, enabling inducible nuclear translocation and activation upon estradiol treatment. An analogous vector expressing Zbtb20, minus its DNA-binding Zinc Finger domain (ΔZF), fused to ER, was used to assess the dependence of Zbtb20 function on direct DNA binding. We introduced these vectors into the P3 plasma cell line, which expresses little endogenous Zbtb20. Two clones were generated for each construct. Ectopic expression of Zbtb20 and translocation of Zbtb20 to the nucleus upon estradiol treatment were confirmed (Fig. 2 C and not depicted).

Microarray screens were performed with the P3 cell lines 6 and 48 h after estradiol treatment to identify Zbtb20 regulated genes. Ingenuity Pathway Analysis revealed that the cell cycle and life span pathways were most affected by increased Zbtb20 expression in P3 cells (unpublished data). Genes controlling proliferation, such as cyclin-dependent kinases (CDKs) p15, p16, p21, and cell survival genes including *Bcl-w* and *Pim2*, were most affected among the array probes (Fig. 3 A). Quantitative PCR analyses suggested that the main CDK regulated by Zbtb20 is p15 (Fig. 3 B). We performed in vitro proliferation assays to determine whether the modulation of cell cycle regulators by Zbtb20 had a biological impact on the cells. The different clones of P3 cells were cultured (±estradiol) and the cells counted daily. Strikingly, when Zbtb20 was induced in P3/Zbtb20-ER cells, their numbers decreased significantly

Published April 7, 2014

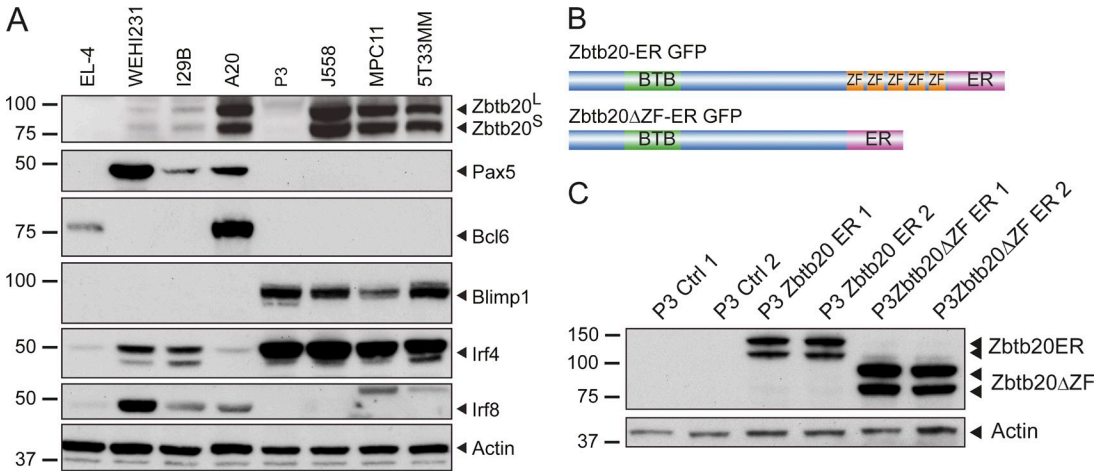

Figure 2. Generation of Zbtb20 monoclonal antibody and Zbtb20 inducible cell lines. (A) Western blot analyses of Zbtb20, Pax5, Bcl6, Blimp1, Irf4, Irf8, and actin expression in the indicated cell lines. Representative of at least two independent experiments. (B) Schematic representation of the Zbtb20-ER and Zbtb20ΔZF-ER inducible vectors. The BTB domain, the five zinc finger domains, and the ER sequence are depicted. (C) Western blot analyses to assess Zbtb20 and actin expression in the different clones of P3 stably transduced with the control vector, Zbtb20-ER, or Zbtb20ΔZF-ER. Representative of three independent experiments.

over time compared with controls. DNA binding was required for the response (Fig. 3 C). We performed cell cycle analyses and found that reduced proliferation in P3/Zbtb20-ER cultures correlated with an increased percentage of cells in the G1 phase of the cycle. Kinetic experiments revealed that upon introduction to culture, ~50% of untreated P3/Zbtb20-ER cells quickly left G1 to enter the G2, M, and S phases, whereas Zbtb20 induction detained cells in G1 (Fig. 3 D).

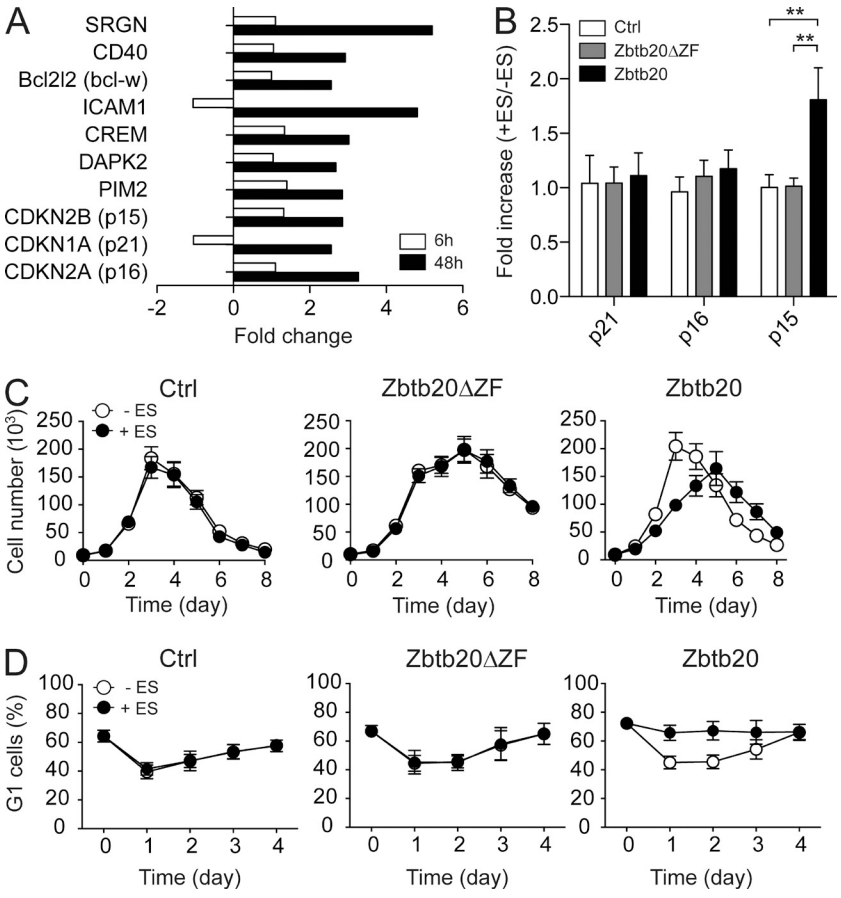

Figure 3. Effect of Zbtb20 induction on proliferation in P3 cells stably transduced with an inducible form of Zbtb20. (A) Fold change of indicated genes involved in the canonical cellular growth and proliferation pathway (Ingenuity Pathway Analysis) found by microarray to be modulated after 6 and 48 h of estradiol (ES) treatment of P3 cells stably expressing Zbtb20-ER. Data are from two independent experiments. (B) Fold increase of the indicated cell survival genes after 48 h of culture ± ES in P3 cells transduced with the indicated vectors, as assessed by qPCR. Bars represent mean ± SD of three independent experiments, each performed in duplicate. From left to right: **, P = 0.0019; **, P = 0.0022. (C) Absolute cell numbers of P3 cells expressing the indicated constructs at the time points shown ± ES. Circles represent mean ± SEM of three independent experiments in triplicate. Statistical differences between curves was assessed using the growth curve analysis method (Mirman et al., 2008) Ctrl, P = 0.94; Zbtb20ΔZF, P = 0.92; Zbtb20, P = 0.19. (D) DNA content of P3 cells transduced with the indicated vectors cultured in presence or absence of ES was assessed by flow cytometry. The percentage of cells in G1 phase at the indicated time points is represented. Circles represent mean ± SD of three independent experiments in triplicate. Statistical differences between curves was assessed as in (C). Ctrl, P = 0.99; Zbtb20ΔZF, P = 0.79; Zbtb20, P = 3×10^9.

Published April 7, 2014

Quantitative PCR was also performed to confirm the Zbtb20-mediated effect on expression of survival genes identified by microarray. *Bcl-w*, *Mcl-1*, *Bcl-x*, *Pim2*, *Bcma* (*Tnfrsf17*), and *Bcl2* were indeed induced by Zbtb20 in the plasma cell line (Fig. 4 A), and in all cases required the Zbtb20 DNA-binding domain (Fig. 4 A). To determine whether Zbtb20 induction confers resistance to stress-induced cell death, the P3 clones were cultured for 48 h (±estradiol) and subsequently exposed to the DNA damage–inducing agents etoposide or adriamycin for 24 h. Both of these drugs caused a strong increase in cell death accompanied by caspase 3 activation in the control cell lines (Fig. 4, B and C). Upon Zbtb20 induction, the percentages of both PI^+ and active caspase 3^+ cells were significantly reduced, showing that Zbtb20 can promote cell survival (Fig. 4, B and C). To determine whether the modulation of survival mediated by Zbtb20 is restricted to P3 cells, or can be generalized to other cell types, we overexpressed Zbtb20 in the immature WEHI231 B cell lymphoma and the plasmacytoma MPC11. The modulation of plasma cell genes was assessed by qPCR. Inducing Zbtb20 in WEHI231 did not affect cell survival or cell cycle gene expression. However, in the plasmacytoma cell line MPC11, the induction of Zbtb20 led to similar effects as in the P3 cell line (Fig. 4 D and not depicted). These results suggest that Zbtb20 is a potential cell stage–specific modulator of cell cycle and cell survival through the regulation of key genes involved in these critical processes.

Zbtb20 promotes plasma cell differentiation in primary B cells

To ask whether Zbtb20 could influence gene expression and differentiation in primary B cells, we generated a constitutively active Zbtb20 retroviral vector coexpressing mCherry and infected LPS activated splenic B cells from *Blimp1*$^{gfp/+}$ reporter mice. Zbtb20 overexpression strongly accelerated the differentiation of B cells into Blimp1/GFP^+ plasma cells, which were also syndecan-1^+ and $MHCII^{lo}$ and secreted Ig (Fig. 5, A–C). $mCherry^+$ cells harvested from LPS cultures 3 d after infection with control or Zbtb20 retroviruses were sorted and the expression of several genes was measured. As expected, the

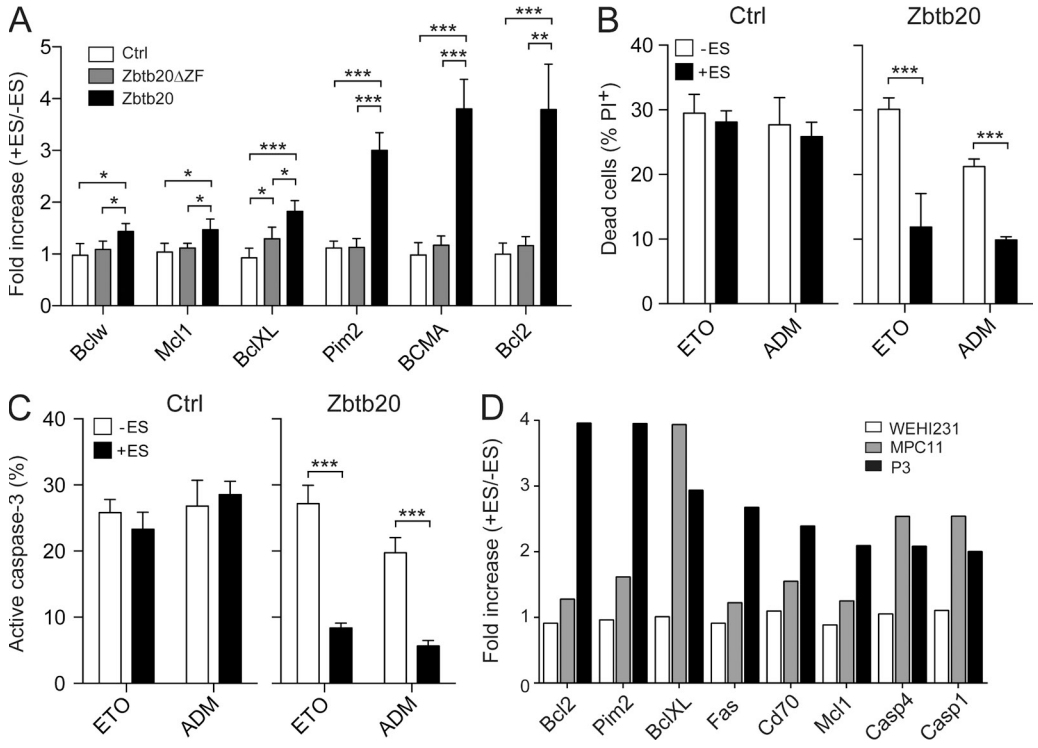

Figure 4. Effect of Zbtb20 induction on cell survival in P3 cells stably transduced with an inducible form of Zbtb20. (A) Fold increase of the indicated cell survival genes after 48 h of culture ± estradiol (ES) in P3 cells stably transduced with the indicated vectors, as assessed by qPCR. Bars represent mean ± SD from three independent experiments, each performed in duplicate. From left to right: *, P = 0.0151; *, P = 0.0197; *, P = 0.0167; *, P = 0.0185; *, P = 0.0473; ***, P = 0.0007; *, P = 0.0138; ***, P < 0.0001; ***, P < 0.0001; ***, P < 0.0001; ***, P = 0.0001; ***, P = 0.0008; and **, P = 0.0010 (Student's *t* test). (B) FACS analysis using PI staining to assess dead cells 24 h after culture of P3 cell line stably transduced with the indicated vectors in presence of the indicated drug (Eto, etoposide; ADM, adriamycin). Cells were pretreated for 48 h with estradiol. Bars represent mean ± SD of the percentage of dead cells, normalized to untreated cells. Data are from four independent experiments, each performed in duplicate. From left to right: ***, P < 0.0001; ***, P = 0.0004. (C) Intracellular FACS analysis for the active form of caspase-3 15 h after culture in presence of the indicated drug (ETO, etoposide; ADM, adriamycin). Cells were pretreated for 48 h with ES. Bars represent mean ± SD, normalized to untreated cells, from four independent experiments. From left to right: ***, P = 0.0005; ***, P = 0.0008. (D) Fold increase of the indicated cell survival genes after 48 h of culture ± estradiol (ES) in P3 cells stably transduced with the Zbtb20-ER vector, as assessed in an apoptosis qPCR array. Data are representative of two independent experiments.

Published April 7, 2014

Zbtb20 vector drove high *Zbtb20* expression (Fig. 5 D). Other critical plasma cell regulators, such as *Blimp1*, *Irf4*, and *Xbp1* were also induced, whereas *Ciita* and *Bcl6* were reduced. These results identify Zbtb20 as a facilitator of plasma cell differentiation, increasing the probability of *Blimp1* induction in activated B cells.

To determine whether Zbtb20 is able to rescue plasma cell differentiation in Blimp1- or Irf4-deficient B cells, we overexpressed Zbtb20 in LPS-activated mutant B cells in vitro. As shown in Fig. 5 (E and F), Zbtb20 increased the percentage of cells that expressed Blimp1/GFP both in the absence of functional Blimp1 protein (14.4 ± 3.8% for vector controls compared with 20.0 ± 3.4% for Zbtb20-transduced cells; $n = 4$; $P = 0.003$) and in the absence of Irf-4 (47.0 ± 8.2% for controls vs. 58.3 ± 3.6% for Zbtb20-transduced cells; $n = 4$; $P = 0.02$). These Blimp1/GFP$^+$ cells were also syndecan-1$^{-/lo}$, and correspond to the immature preplasmablasts described previously (Kallies et al., 2007). Zbtb20 was not able to drive differentiation to the mature syndecan-1$^+$ plasmablast stage and could not induce or increase the antibody secretion in either mutant (Fig. 5, E and F; and not depicted). Thus, while Zbtb20 facilitates *Blimp1* induction and initiation of differentiation, it is not sufficient to trigger full plasma cell differentiation in the absence of Blimp1 or Irf4.

Zbtb20 is required for a normal humoral immune response

To assess the function that Zbtb20 plays in the B cell compartment in vivo, and to circumvent the fact that Zbtb20 KO mice die perinatally, we reconstituted sublethally irradiated *Rag1*$^{-/-}$ or *Rag2*$^{-/-}$/$\gamma c^{-/-}$ mice with fetal liver cells from Zbtb20 KO (Rosenthal et al., 2012) or WT littermate embryos. Analysis of the B cell compartment revealed normal cell populations in the spleen and BM of mice from both groups (unpublished data). B1 cells in the peritoneal cavity, which normally express Zbtb20, were found at normal levels in the mutants (Fig. 6 A). However, using the Blimp1/GFP reporter, we found that the elevated Blimp1 levels that are characteristic of normal B1 cells (Fairfax et al., 2007) were not maintained

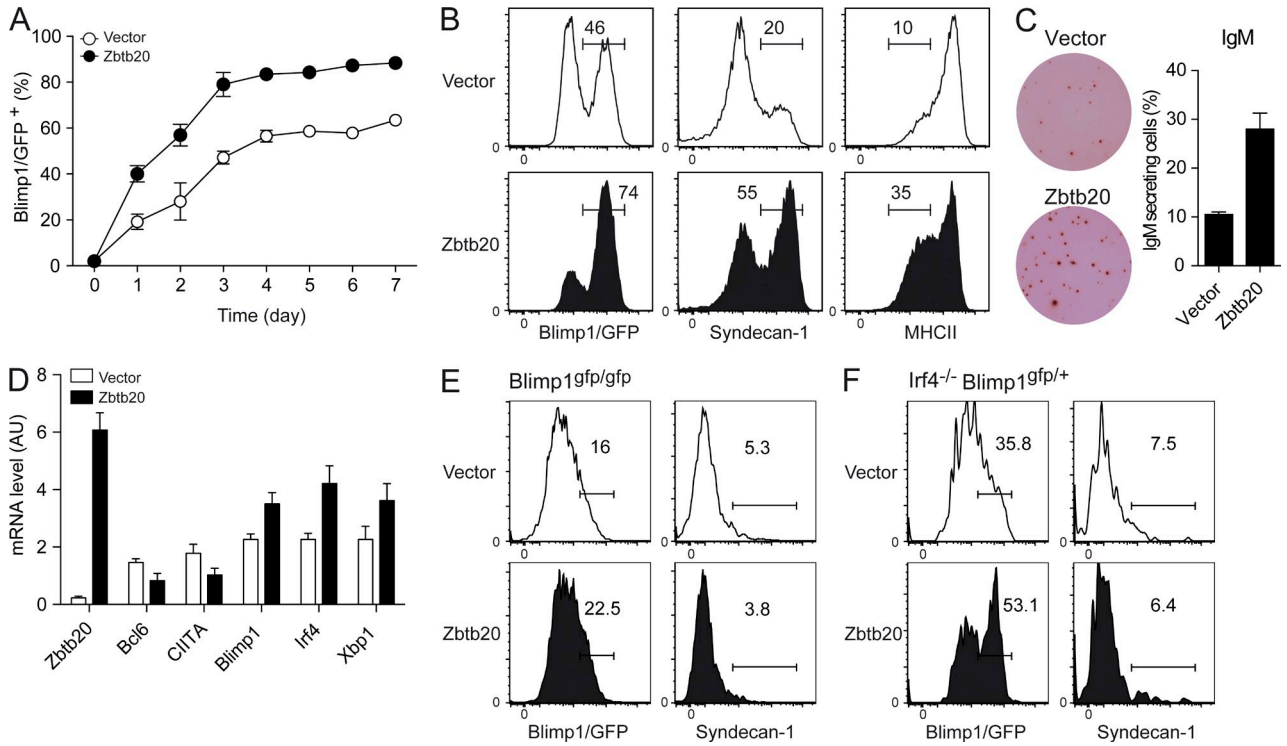

Figure 5. Zbtb20 promotes plasma cell differentiation in primary B cells. (A) Purified B220$^+$ *Blimp1*$^{gfp/+}$ cells were cultured for 24 h with LPS and transduced with a control or Zbtb20-encoding vector expressing mCherry as a reporter. The percentage of Blimp1/GFP expressing cells among the mCherry$^+$ cells was assessed at the indicated times. Circles represent mean ± SD from three independent experiments. (B) 48 h after transduction, mCherry$^+$ cells were analyzed for the expression of Blimp1/GFP, syndecan-1, and MHCII. The percentage of cells in each gate is indicated. Data are representative of six independent experiments. (C) mCherry$^+$ cells were sorted on day 2 after retrotransduction and analyzed by ELISpot for the frequency of IgM-secreting cells. Bars represent mean ± SD of three independent experiments. (D) mCherry$^+$ cells were sorted on day 2 after retrotransduction and assessed by qPCR for expression of Zbtb20 and genes involved in plasma cell differentiation. Results are presented relative to *hmbs* mRNA as mean ± SD of three independent experiments. (E) Blimp1-deficient B220$^+$ cells were transduced with a control or Zbtb20-encoding vector. After 3 d, transduced cells were analyzed for the expression of Blimp1/GFP and syndecan-1 expression among mCherry$^+$ cells. The percentage of cells in each gate is indicated. Data are representative of three independent experiments. (F) *Irf4*$^{-/-}$ Blimp1/GFP reporter B220$^+$ cells were transduced with a control or Zbtb20-encoding vector. After 3 d, transduced cells were analyzed for Blimp1/GFP and syndecan-1 expression among mCherry$^+$ cells. Data are representative of three independent experiments.

Published April 7, 2014

in Zbtb20-deficient cells (Fig. 6 A), and that, when cultured in vitro with LPS or CpG, Zbtb20-deficient B1 cells differentiated less efficiently into syndecan-1$^+$ ASCs than WT B1 cells (Fig. 6 B). Total serum immunoglobulin levels in naive mice, measured by Igκ ELISA, were reduced by 4–5-fold in Zbtb20-deficient mice (18.4 ± 2.8 mg/ml for WT compared with 3.9 ± 0.4 mg/ml for mutants; n = 4 for each), with reductions across all isotypes tested (Fig. 6 C and not depicted). ASC numbers in naive mice, estimated by ELISpot, were also significantly reduced (Fig. 6 C).

We immunized reconstituted WT and Zbtb20 KO mice with NP-KLH to determine whether Zbtb20 KO mice were

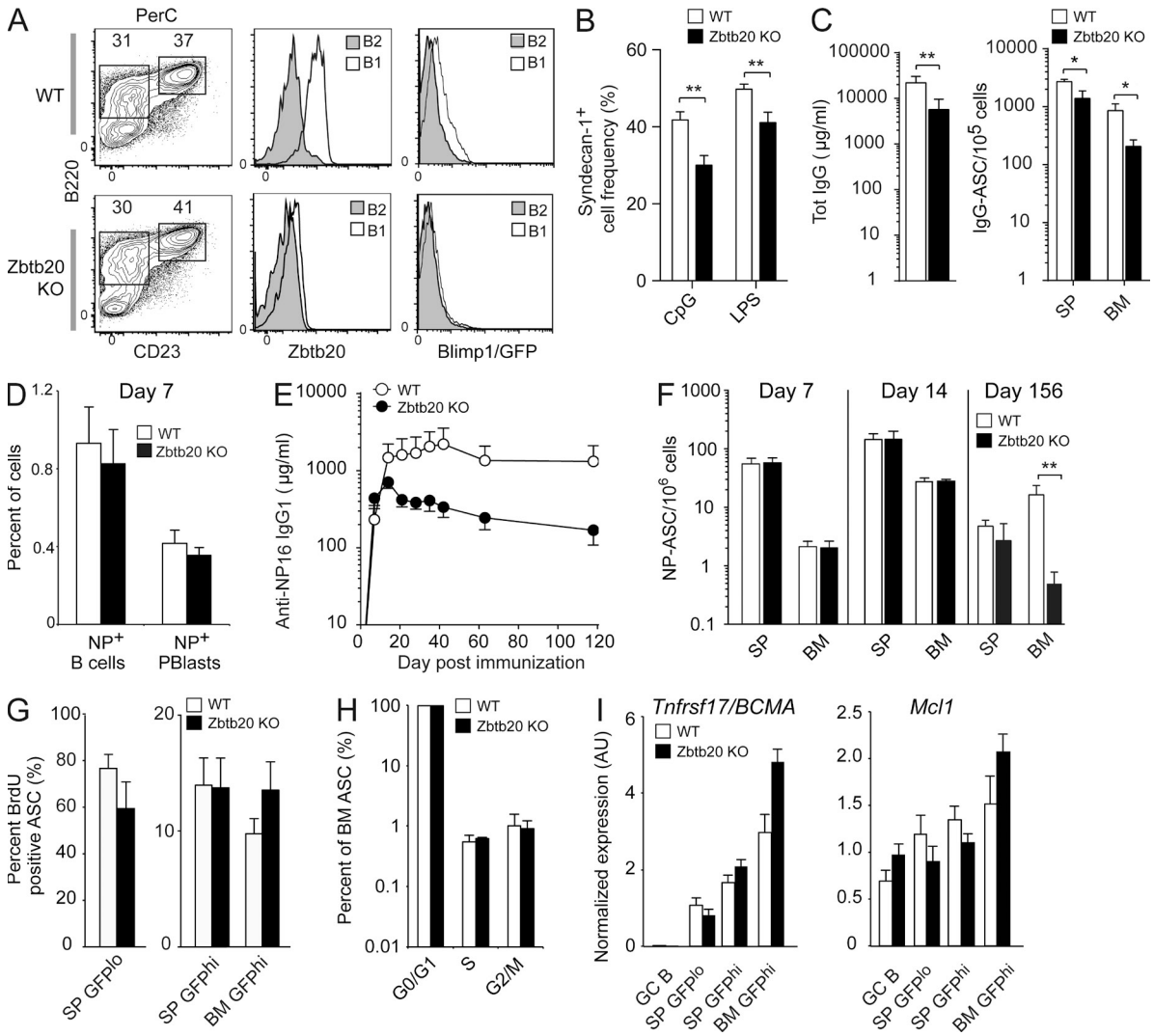

Figure 6. Defective B cell response in Zbtb20 KO mice. (A) Flow cytometric analyses of peritoneal cavity (PerC) cells to determine the percentage of B1 (B220^{int}, CD23$^-$) and B2 (B220$^+$ CD23$^+$) cells from WT and Zbtb20 KO mice expressing the Blimp1 GFP reporter. Intracellular staining shows the level of Zbtb20 in each of these populations, and Blimp1 levels are shown using the GFP reporter. Results are representative of at least two independent experiments using three mice of each genotype. (B) B1 cells from WT and Zbtb20 KO mice were cultured with CpG or LPS for 2 d. The percentage of syndecan-1$^+$ cells was assessed by flow cytometry. Bars represent the mean ± SD from seven mice analyzed in three independent experiments. **, P = 0.0065; **, P = 0.0052. (C) Total serum Ig (measured as Igκ) in naive mice, and ASCs as determined by Igκ ELISpot. Bars represent the mean ± SD from three independent experiments, each using two mice. **, P = 0.0043; *, P = 0.0329; *, P = 0.0257. (D) Analysis of spleen cells 7 d after NP-KLH immunization in WT and Zbtb20 KO mice. Cells were gated as B220$^+$ lymphocytes or as Blimp1/GFP^{lo} plasmablasts, and the level of NP staining was assessed on the gated cells. Data are representative of five to six mice per genotype analyzed in two independent experiments. (E) Titers of NP-specific IgG1 in serum of immunized WT (n = 4) or KO (n = 5) mice over ∼4 mo. Bars represent mean ± SD. Representative of two independent experiments. (F) NP-specific IgG1 ASCs identified by ELISpot assay in spleens and BM of mice at the times indicated. Bars represent mean ± SD (n = 3 to 5 mice for each group). Representative of two independent experiments. *, P = 0.03, calculated using the Mann-Whitney U test. (G) Sorted ASCs were stained for BrdU incorporation. Bars represent mean ± SD from three mice per genotype and data are representative of two independent experiments. (H) Cell cycle analysis of sorted ASCs. Bars represent mean ± SD from three mice per genotype and data are representative of two independent experiments. (I) qPCR on sorted plasma cell populations for the indicated genes. Bars represent mean ± SD from three mice per genotype and data are representative of two independent experiments.

Published April 7, 2014

able to generate normal humoral immune responses. GCs developed similarly in the presence or absence of Zbtb20 (5.6 ± 1.2% of $B220^+$ cells for WT compared with 5.3 ± 1.2% for mutants at day 7) and were maintained at similar level up to 21 d after immunization (unpublished data). The percentages of centroblasts and centrocytes in the GCs, and of apoptotic GC B cells in spleen, were not affected by Zbtb20 loss (unpublished data). NP-specific B cells ($B220^+$/BlimpGFP$^-$) and plasmablasts (Blimp1/GFP^{lo}) were detected at day 7 in similar numbers in mice of both genotypes, indicating that the initial response to immunization was not impacted by Zbtb20 loss (Fig. 6 D). At this early time point, the GC response is only just beginning, so these data imply that the extrafollicular ASC response is intact in the mutants. Initially, serum anti-NP IgG1 titers were also similar between KO and WT mice (Fig. 6 E), and the frequencies of ASCs secreting high-affinity anti-NP IgG1 antibody were comparable (unpublished data), indicating normal affinity maturation in Zbtb20-null mice. Strikingly, however, the KO mice were unable to achieve the same anti-NP antibody titers as controls at the height of the response (peaking at ∼5-fold lower levels than controls). Furthermore, whereas WT mice retained high anti-NP IgG1 titers for the duration of the experiment, titers in KO mice declined markedly from the lower peak, and finished more than eightfold lower than in WT mice (Fig. 6 E). Interestingly, although the frequencies of NP-specific ASCs in spleen and BM were equivalent on day 14 in WT and KO mice, at later time points (days 118 [not depicted] and 156 [Fig. 6 F]), the KO mice had significantly (>30-fold) fewer ASCs in BM than controls. ASC numbers in the spleens of KO mice were also consistently reduced (to ∼60% of WT levels), but the difference did not reach statistical significance (Fig. 6 F). These in vivo results indicate that, under this immunization regimen, that Zbtb20 is not essential for an initial GC, plasma cell, and antibody response. However, in its absence, the early antibody response is blunted and, later, ASC loss in the BM is significantly and specifically accelerated, causing serum Ig levels to wane more rapidly.

We performed several experiments to further characterize the difference between ASCs in WT and KO mice. Antigen-specific ASCs lose antigen receptor expression upon differentiation, as observed using the Blimp1/GFP reporter gene. It is therefore not possible to distinguish recently generated from long-lived ASCs based on surface staining. We therefore measured ASC generation in vivo using BrdU labeling. We did observe the described differences (Kallies et al., 2004) in BrdU incorporation into the cycling splenic Blimp1/GFP^{lo} plasmablasts and the noncycling Blimp1/GFP^{hi} plasma cells of spleen and BM. We did not see significant differences in the percentage of $BrdU^+$ cells in these three populations comparing WT and KO mice, although the KO mice consistently exhibited higher BrdU incorporation in the BM ASC compartment (Fig. 6 G). This is likely to indicate a modest elevation in the influx of recently generate ASCs into the BM, as cell cycle analyses of BM ASCs gave identical results for WT and $Zbtb20^{-/-}$ cells (Fig. 6 H).

We sorted total $syndecan1^+$/Blimp1/GFP^+ plasmablasts and plasma cells from spleen and BM of WT and KO mice and performed qPCR for genes known to be important for ASC longevity, such as *Bcma* and *Mcl1* (O'Connor et al., 2004; Peperzak et al., 2013). These were not reduced in Zbtb20 GC B cells or spleen and BM ASC compared with controls (Fig. 6 I). KO GCs and ASCs also expressed normal levels of *Bcl2*, *Bcl2l1/BclX*, and *Bcl2l11/Bim* compared with their WT counterparts (unpublished data). Together, and with the caveat that we have compared total ASCs from WT and KO mice without knowledge of their ages, these data suggest that Zbtb20 does not strongly affect the generation of ASCs, their capacity to enter a quiescent state, or the expression of known mediators of ASC survival. Zbtb20 is, however, essential for the maintenance of a long-lived antigen-specific BM pool of ASCs and of persistent antigen-specific Ig in serum.

Zbtb20 expression is dependent on Irf4 but independent of Blimp1

To find where Zbtb20 lies in the genetic hierarchy of ASC differentiation, *Blimp1*$^{gfp/+}$ B cells were activated with LPS and Blimp1/GFP-positive and -negative cells were sorted. Both qPCR and FACS analyses consistently showed a slight increase in Zbtb20 expression in GFP^+ *Blimp1*$^{gfp/+}$ control plasmablasts (Fig. 7 A, left; and not depicted). In activated Blimp1-deficient B cells, Zbtb20 expression was higher in the GFP^+ population than in the equivalent control cells (Fig. 7 A, compare middle and left). Blimp1 is therefore not required for Zbtb20 expression; indeed, its loss increases *Zbtb20* expression. As Zbtb20 up-regulates Blimp1 (Fig. 5 A), this implies a complex regulatory relationship between the two repressors. In striking contrast, Irf4 deficiency led to an almost complete loss of Zbtb20 expression in vitro, both in Blimp1/GFP^- and Blimp1/GFP^+ cells (Fig. 7 A).

We then asked whether Zbtb20 expression required Blimp1 or Irf4 in vivo. Because ASCs do not form in the absence of Irf4 or Blimp1, and because GCs require Irf4, we focused on peritoneal B1 cells as a B cell population that expresses Zbtb20 in vivo. B1 cells were evident in mice of each genotype (Fig. 7 B). However, while control and Blimp1-deficient B1 cells expressed Zbtb20, Irf4-deficient B1 cells did not, confirming the Irf4 dependence of Zbtb20 expression in vivo.

We ectopically expressed Irf4 in the mature I29B cell line, which expresses little Irf4 or Zbtb20 (Fig. 2 A), to determine whether Irf4 expression is sufficient for Zbtb20 induction. Enforced Irf4 expression in these cells, confirmed at the mRNA level, provoked an increase in *Zbtb20* mRNA and protein (Fig. 7 C and not depicted). Together, these results indicate that Zbtb20 is critically positioned in the plasma cell transcriptional hierarchy, downstream of Irf4 and in a close but complex relationship with Blimp1.

Irf4 directly binds to a Zbtb20 promoter

Zbtb20 is expressed from a complex gene spanning >750 kbp. RNA sequencing on brain tissue and two cell lines showed that while transcription starts far upstream in the locus in brain,

Published April 7, 2014

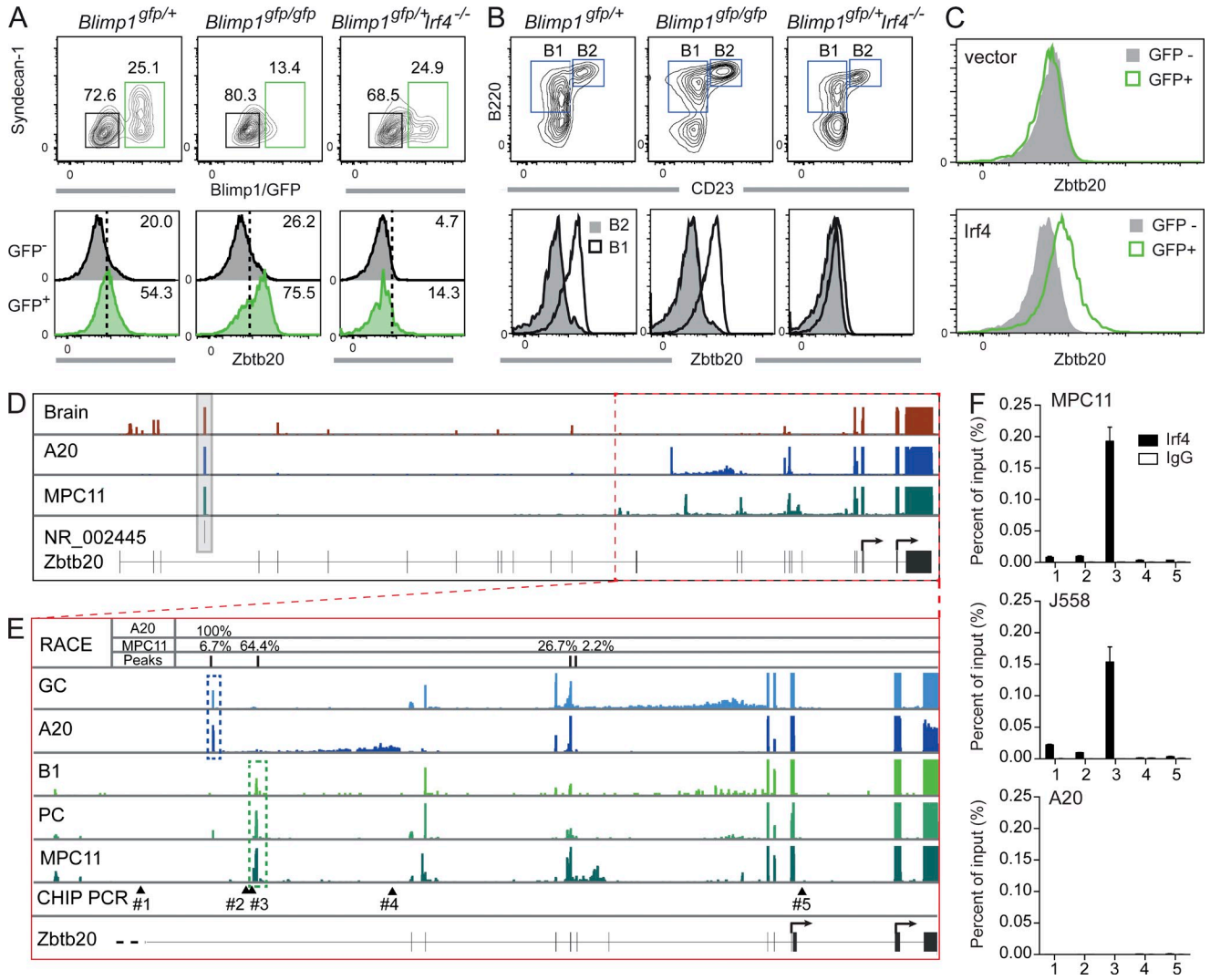

Figure 7. Irf4 binds to the promoter of Zbtb20 to trigger its expression. (A) B cells from the indicated mice were cultured for 3 d with LPS, sorted according to Blimp1/GFP expression and stained for intracellular Zbtb20 levels. Data are representative of three independent experiments on two mice of each genotype. (B) Analysis of peritoneal cells of the indicated mice to identify B1 and B2 cells. Histograms show Zbtb20 levels for both populations. Representative of three independent experiments, with three mice for each genotype. (C) I29B cells were transduced with an Irf4/GFP or a control vector and sorted at day 3 according to GFP level. Zbtb20 levels were assessed by FACS. Representative of three independent experiments. (D) RNA-Seq analysis of brain tissue, A20, and MPC11. Structure of the Zbtb20 gene according to the Ensembl database is depicted. The presence of gene NR_002445 is indicated (gray box). Arrows shows alternative Zbtb20 translational start sites (TSS). Representative of one experiment. (E) Identification of Zbtb20 transcriptional start sites in MPC11 and A20 cells by 5′RACE PCR. 18 independent clones from A20 and 45 clones from MPC11 cell lines were bidirectionally sequenced. Their location and frequency among the sequenced clones are shown. RNA-Seq was performed on the indicated cell lines and primary B cells. Putative transcriptional start sites in GC (blue dotted box) and ASC/B1 (green dotted box) are indicated. Locations of sequences (#1–5; arrowheads) containing putative Irf4 binding sites are depicted. (F) Anti-Irf4 ChIP was performed on the indicated cell lines and assessed by qPCR using primers 1–5 listed in Table S5. Data are representative of two independent experiments.

in the GC-like A20 lymphoma and MPC11 plasmacytoma, transcripts were restricted to downstream regions of the locus (boxed in Fig. 7 D). 5′ RACE on A20 and MPC11 identified two major and distinct start sites from as yet unmapped exons (Fig. 7 E). RNA sequencing on ex vivo purified B1, GCs and plasma cells showed profiles of Zbtb20 expression matching their cell line counterparts, with peaks in these new exons (Fig. 7 E). Thus, Zbtb20 is differentially regulated in GCs and B1/ASCs.

Computational analyses (TransFacPro) identified putative Irf4 binding sites near the B1/ASCs Zbtb20 transcriptional start site and elsewhere in the locus (Fig. 7 E). Chromatin immunoprecipitation from two plasmacytomas (MPC11 and J558) with anti-Irf4 antibody showed a strong enrichment of sequences preceding the B1/ASCs transcriptional start site, but not of other putative Irf4 binding sites (Fig. 7 F). No enrichment was seen in Irf4 ChIP with the GC line A20, which does not express Irf4. Thus, Zbtb20 is regulated

Published April 7, 2014

differentially in GC B cells and ASCs, with Irf4 directly activating the gene from a newly identified plasma cell-specific promoter.

DISCUSSION

Terminal B cell differentiation is a complex process currently modeled upon the actions of a small number of "master regulators," and the gaps in our understanding are clear. Insight into the mechanism of differentiation, both its initiation and its full execution, is advanced with the identification of each new contributing factor.

Here, we identify Zbtb20 as a new mediator of B cell differentiation specifically expressed in B1 and GC B cells and ASCs. Zbtb20 is a BTB-ZF transcription factor, and other members of the family have been shown to be active within the B cell lineage (Chevrier and Corcoran, 2014). For instance, early B lineage commitment is mediated by LRF, Bcl6, and Miz-1 (Maeda et al., 2007; Duy et al., 2010; Kosan et al., 2010), MZ B cell differentiation is controlled by LRF (Sakurai et al., 2011), and the GC reaction is driven by Bcl6 and LRF (Fukuda et al., 1997; Sakurai et al., 2011). Finally, Zbtb32 has been associated with plasma cell differentiation (Yoon et al., 2012).

In activated conventional B cells, which express little Zbtb20, its enforced expression increased *Blimp1* induction and strongly promoted plasma cell differentiation. In contrast, Zbtb20 is constitutively expressed in B1 cells. These sentinel cells of the peritoneal and pleural cavities rapidly differentiate to ASCs upon antigen encounter. They are transcriptionally poised toward differentiation, with elevated *Blimp1* and depressed *Pax5* and *Bcl6* levels compared with conventional B cells (Fairfax et al., 2007). We show that Zbtb20 is highly expressed in B1 cells, where it facilitates *Blimp1* expression in vivo and efficient ASC differentiation in vitro. Interestingly Zbtb32, which has recently been shown to influence plasma cell differentiation (Yoon et al., 2012), is also highly expressed in B1 cells (unpublished data). These data suggest that Zbtb20 and Zbtb32 may contribute to the special characteristics of B1 cells. Interestingly, MZ B cells, which are also able to rapidly differentiate into ASCs in vitro, express low levels of both Zbtb20 and Zbtb32 (Fig. 1 A and not depicted). Therefore, in this B cell subpopulation, rapid activation and differentiation is likely to depend on a different transcriptional pathway. For example, MZ B cells do not down-modulate *Pax5* or *Bcl6* levels as strongly as B1 cells do (Fairfax et al., 2007; and unpublished data). The difference in cell behavior is also consistent with the fact that B1 and MZ B cells have different developmental precursors and differential requirements for key transcription factors, such as Oct2, Obf-1, and LRF, for their generation (Humbert and Corcoran, 1997; Samardzic et al., 2002; Sakurai et al., 2011).

The effects of Zbtb20 on plasma cell differentiation, cell cycle arrest, and cell survival are opposite to the role played by Bcl6. BTB-ZF transcription factors are known to be able to heterodimerize through their BTB domains (Costoya, 2007) and part of the function played by Bcl6 in GC depends on its interaction with the BTB-ZF transcription factor Miz1 (Phan et al., 2005; Saito et al., 2009). Due to its high expression in GC, Zbtb20 would be an obvious candidate to counteract Bcl6 function and promote GC exit. However, our in vivo data using NP-KLH immunization did not identify a role for Zbtb20 in the generation of the GC, in the switch between dark zone and light zone, or in the frequency of apoptotic cells. Alternatively, Zbtb20 may oppose the repressive influence of Bcl6 on *Blimp1* expression and initiation of ASC differentiation. Because we have not observed physical interactions between Zbtb20 and Bcl6 or Miz1 (unpublished data), this is unlikely to be via direct binding between Zbtb20 and Bcl6, but may reflect competition for binding to common gene targets. Thus far, the function Zbtb20 plays in GC remains elusive and requires further investigation.

Zbtb20 is expressed at its highest level in mature, nondividing, long-lived plasma cells in vivo. In transformed plasma cells, Zbtb20 increased expression of genes known to be critical for ASC survival in vivo, such as *Bcma* and *Mcl1* (O'Connor et al., 2004; Peperzak et al., 2013), and promoted survival to cytotoxic agents. It also induced expression of the CDK inhibitor p15, leading to cell cycle blockade. Interestingly, other reports have linked BTB-ZF proteins to the regulation of CDK inhibitors (Phan et al., 2005; Weber et al., 2008; Jeon et al., 2009). Collectively, our in vitro data suggest that Zbtb20 may act to repress mitosis and promote the survival of plasma cells. In vivo, loss of Zbtb20 did not dramatically affect induction of antigen-specific plasma cells, isotype switching, affinity maturation, or the migration of plasma cells to the BM. However, the persistence of antigen-specific plasma cells, as measured by their output in the serum and their maintenance in the BM (and to a lesser extent in the spleen), was significantly reduced in the absence of Zbtb20.

In primary ASCs taken ex vivo, expression of *Bcma* and *Mcl1*, two potent mediators of plasma cell survival (O'Connor et al., 2004; Peperzak et al., 2013) was not affected by the absence of Zbtb20. Similarly, BrdU labeling and cell cycle analysis did not reveal a dramatic effect of Zbtb20 on ASC cell cycle parameters. There was a suggestion that the BM pool of *Zbtb20*$^{-/-}$ ASCs contained more newly generated cells, which could account for the observed depletion of antigen-specific ASCs in the *Zbtb20*$^{-/-}$ BM pool. Manz et al. (2005) describe competition for limited survival niches in the BM between existing and newly generated plasma cells. If the number of new ASCs entering the BM is elevated in Zbtb20 deficiency, possibly as a result of its role in modulating cell cycle or cell survival genes in the short term, the newcomers may replace the antigen-specific ASC induced by immunization more rapidly than in normal mice. The observation would have to be confirmed through the tracking of ASCs from their generation until their death, which is currently technically challenging. To fully understand how Zbtb20 affects ASC maintenance, it will be necessary to identify its direct targets in plasma cells. In addition, because our in vitro studies indicated that the effect of Zbtb20 on cell survival is context dependent, it is likely that this effect requires as yet unidentified cofactors of Zbtb20, expressed in ASCs but not B cells.

Published April 7, 2014

A recent study showed that Pax5 binds in the Zbtb20 promoter, which suggests that Pax5 could contribute to Zbtb20 silencing in immature B cell type (Revilla-I-Domingo et al., 2012). This concurs with our observation that Zbtb20 is not expressed during B cell development. However, because the presence of Pax5 in GCs, B1, and early plasma cells does not prevent Zbtb20 expression, Pax5 is not sufficient to repress Zbtb20. We show here that Zbtb20 induction is dependent on Irf4 in B1 cells and during plasma cell differentiation. We mapped two new transcriptional start sites, one specifically active in plasma cells and B1 cells and the other in GC B cells, in newly described exons. B1 and ASCs share a Zbtb20 promoter that contains a Pu-1/Irf4 consensus site to which Irf4 binds in vivo. We propose that direct binding of Irf4 to this site drives Zbtb20 expression in B1 and ASCs. Given the absence of Irf4 in GC B cells, induction of *Zbtb20* in GCs likely acts through other factors.

The relationship between *Blimp1* and *Zbtb20* expression is more perplexing. We show that Zbtb20 overexpression increases the number of Blimp1-expressing B1 cells in vivo and in culture. We also show that, in the absence of Blimp1, *Zbtb20* is expressed normally in B1 cells, but in in vitro activated cells, its expression increases. This implies that Zbtb20 is upstream of Blimp1 and favors its expression, but that Blimp1 may be part of a negative feedback loop that regulates Zbtb20. Consistent with this, ChIP sequencing analyses showed that Blimp1 associates directly with the *Zbtb20* locus both in mouse (unpublished data; M. Minnich and M. Busslinger, personal communication) and human, via a highly conserved domain (unpublished data; R. Tooze, personal communication). Although the expression of Ztbb20 in human plasma cells is not clear yet, this observation suggests that a similar pattern is shared between mice and human. Since Zbtb20 is expressed in certain human B cell lymphomas, it will be of interest to further investigate the exact expression pattern of Zbtb20 in the human B cell lineage.

In summary, our study has identified Zbtb20 as a new regulator of plasma cell differentiation. It is expressed in ASCs and their direct precursors and is Irf4 dependent. Zbtb20 has the capacity to impact several phenotypic properties of activated B cells, plasmablasts and mature plasma cells, including enhancing differentiation, slowing cell division, and bestowing ASC longevity via enhanced survival. Therefore, our data provide new insights into plasma cell biology and open the way to a more detailed analysis of the roles Zbtb20 plays in the fine-tuning of plasma cell differentiation and the maintenance of long-term humoral immunity.

MATERIALS AND METHODS

Mice. Previous reports have described the *Blimp1*$^{gfp/+}$ (Kallies et al., 2004), the *Irf4*$^{-/-}$ (Mittrücker et al., 1997), and the Zbtb20 KO (Rosenthal et al., 2012) mice. Zbtb20 KO mice were generated by reconstituting sub lethally irradiated *Rag1*$^{-/-}$ or *Rag2*$^{-/-}\gamma c^{-/-}$ mice (The Jackson Laboratory) with fetal liver cells of day 13.5 embryos. Mice were used after at least eight weeks of reconstitution, at which time B and T cells were apparent in peripheral blood at normal and equivalent percentages in Zbtb20 WT and KO recipient mice. Consistent with the low dose irradiation, lymphoid and myeloid populations in the BM were indistinguishable between the groups (using markers for myeloid and erythroid cells and megakaryocytes: anti-B220, CD4, CD11b, CD11c, Ly6G, Ter119 and CD41, respectively). All mice were maintained on a C57BL/6 background at the specific pathogen–free facilities of The Walter and Eliza Hall Institute, and experiments were undertaken according to this institution's Animal Ethics Committee guidelines and approval (#AEC2010.010).

Immunization. Immunization was a single i.p. injection of 100 µg 4(hydroxy-3)-nitrophenyl acetyl (NP) coupled to keyhole limpet hemocyanin (KLH) at a ratio of 20:1, precipitated onto alum, and washed extensively before injection. Alternatively, mice were injected i.p. with 2×10^8 sheep red blood cells (Applied Biological Products Management).

Cell culture and retroviral complementation. EL4, WEHI231, I29B, A20, P3.6.2.8.1, J558, 5T33MM, and MPC11 cell lines were generated in house or obtained from the American Type Culture Collection. Primary B cells were isolated from the spleens of 5–8-wk-old C57BL/6 mice and purified using anti–B220-coupled magnetic beads (Miltenyi Biotec) with purity typically superior to 95%. Cells were cultured in DME complemented with 10% FCS, 2 mM L-Glutamine, 0.1 mM L-Asparagine, nonessential amino acids (Sigma-Aldrich), and 50 µM 2-mercaptoethanol. Primary B cells were activated with 10 µg/ml LPS. Where indicated, cells were spin infected with retroviral supernatant as previously described (Bahnson et al., 1995). P3 were retrotransduced with the inducible pMXpie-Zbtb20-ER-ires-GFP or pMXpie-Zbtb20ΔZF-ER-ires-GFP vectors or the pMXpie-ires-GFP control vector. Puromycin-resistant clones were selected for high GFP expression. Nuclear translocation of ER-fused proteins was induced by the addition of 1 µM β-estradiol (ES). For cell death assays, cells were cultured with 5 µM etoposide (Sigma-Aldrich) or 5 µM adriamycin (doxorubicin; Sigma-Aldrich). Primary B cells were spin infected with the pMSCV-ires-mCherry or pMSCV-Zbtb20-ires-mCherry expression vectors. Spin infection was performed 24 h after in vitro activation, and cells were then returned to culture in the same medium.

Microarray. Total RNA was prepared from resting follicular B cells and ex vivo splenic and BM plasma cells (isolated from *Blimp1*$^{gfp/+}$ reporter mice) using RNeasy Mini kits (QIAGEN). Three biological replicate RNA samples from each experimental group were hybridized to Illumina MouseWG-6 v2 Expression BeadChips. Probe intensity profiles exported from BeadStudio were analyzed with the limma and Illumina software packages (Gentleman et al., 2004) using the manufacturer's probe annotation (released November 2008; Illumina). Raw intensities were normexp background correction using negative control probes, quantile normalized, and log2 transformed (Shi et al., 2010). Differential expression was assessed using linear models and empirical Bayes moderated t-statistics (Smyth, 2004). P-values were adjusted using the Benjamini and Hochberg algorithm to control the false discovery rate (FDR). Genes with FDR ≤ 0.05 were considered differentially expressed. Known pathways and gene networks were superimposed on the differential expression results using Ingenuity Pathway Analysis (Ingenuity Systems). The array data can be found at the NCBI database under GEO accession no. GSE43214.

Quantitative RT-PCR. First strand cDNA synthesis and quantitative RT-PCR analysis were performed as described previously (Emslie et al., 2008). Primer sequences are supplied in Table S1. When indicated, qPCR were performed using the apoptosis qPCR array (SA Biosciences).

mAb generation and Western blot. An anti–Zbtb20 mAb was generated in rats by immunization with a purified hexahistidine–Zbtb20 fusion protein consisting of 223 aa lying between the BTB and the zinc finger domains of mouse Zbtb20. Cells of interest were lysed for total protein extracts or for cytoplasmic and nuclear subcellular fractionation, as previously described (Müller et al., 1989). Antibodies used for Westerns are listed in Table S2.

Published April 7, 2014

Flow cytometry and antibodies. Single-cell suspensions were stained with the antibodies listed in Table S3 in the presence of 2.4G2 mAb to block F_C receptors. Propidium iodide (PI) or Sytox blue (Invitrogen) was used to exclude dead cells. Intracellular staining for Zbtb20 was performed using the Foxp3 Fixation/Permeabilization kit (eBioscience). FACS data were collected using a FACSCanto, LSR II, or Fortessa (all from BD) and analyzed on FlowJo (Tree Star). For cell counts in proliferation assays, beads were added to the cell suspension before analysis. For DNA content analysis, cells were fixed with the eBioscience kit, treated with RNase A for 45 min at 37°C, and stained with PI before FACS analysis. Cell sorting was performed on a MoFlo (Dako), FACSVantage (BD), or FACS Aria (BD) and cell purity was typically >98% upon reanalysis.

Immunohistological analysis. For histological analyses, spleen samples were frozen in OCT (Tissue-Tek; Sakura) and 7-µm sections were stained with anti-B220 (RA3-6B2; biotin, BD), PNA (biotin; Vector Laboratories), and anti-Zbtb20 (4A3; in-house). Detection was performed with anti–rat-Igκ (goat; HRP-conjugated; BD), and streptavidin alkaline phosphatase (Southern-Biotech). The substrates used were as follows: AEC (Vector Laboratories), Fast Blue (Vector Laboratories), and DAB + chromogen (Dako).

BrdU labeling and cell cycle analysis. In vivo BrdU labeling and analysis was performed as described previously, except that mice were fed BrdU water for five rather than four days (Kallies et al., 2004). Cell cycle analysis was performed as described in Zotos et al. (2010).

ELISpot and Elisa. For ELISpot, 500 mCherry$^+$ cells were purified by FACS 2 d after infection and added to a 96-well cellulose ester membrane plate (Millipore) coated with 2 µg/ml DA (sheep anti–mouse Ig; Silenus Laboratories) and incubated for 4–5 h at 37°C and 10% CO_2. IgM secreting cells were identified with anti-IgM (biotin) and streptavidin-AP (Invitrogen). Spots were visualized with BCIP (Sigma-Aldrich) and counted using an automated reader (AID ELISpot Reader System, software version 4). After NP-KLH immunization, spleen and BM total cells were incubated for 5 h on plates previously coated with 20 µg/ml of NP13-BSA. Anti-NP IgG1 was detected using goat anti–mouse IgG1 conjugated to HRP (SouthernBiotech) and visualized as described above. ELISA was performed as described previously (Kallies et al., 2007).

RNA sequencing. RNA was extracted from mouse brain, A20, and MPC11 cell lines and ex vivo from peritoneal B220$^+$/CD23$^-$ B1 cells, follicular B cells (B220$^+$/CD23$^+$) from spleen, BM Blimp-GFP$^+$/syndecan-1$^+$ ASC and splenic PNA$^+$/FAS$^+$/B220$^+$ GC B cells as above. Sequencing (100 bp, paired end) was performed at the Australian Genome Resource Centre, using a HiSeq2000 (Illumina). Reads were mapped to the mouse reference genome mm9 using the Subread aligner (Liao et al., 2013). Ten 16-bp subreads were extracted from each read and mapped without permitting mismatches. A successful hit was reported if three or more subreads from a read mapped to same genomic location. Exon–exon junctions were identified when different subreads from the same read mapped to different exons. Paired-end information was used in the mapping. On average, 94% of reads were successfully mapped. Table S4 gives the percentage of mapped reads for each library. Read depth plots were generated using Integrated Genome Browser (Nicol et al., 2009).

5′ RACE PCR. The transcriptional start site for the mouse Zbtb20 gene was mapped using a RACE cDNA amplification kit (Ambion). Gene-specific nested primers were chosen from a 5′ region of the coding region that is common to both isoforms. PCR products generated from the 5′RACE PCR reaction were purified from an agarose gel and cloned. 18 independent clones from A20 and 45 clones from MPC11 cell lines were bidirectionally sequenced to ensure that microheterogeneities in sequence length were not overlooked.

CHIP PCR. Chromatin immunoprecipitation was performed as previously described (Emslie et al., 2008). In brief, 2×10^7 A20, MPC11 and J558 cells were fixed in 1% formaldehyde and quenched with 10% of glycine 0.25 mM. Sonicated chromatin was precipitated with a goat polyclonal anti-Irf4 antibody (M-17; Santa Cruz Biotechnology, Inc.) or control goat IgG (in-house). Precipitated DNA was assessed by qPCR with the primers indicated in Table S1.

Statistical analysis. Unless otherwise stated, statistical analyses were performed using Prism software. The two-tailed unpaired Student's *t* test was used for statistical analysis. When the normality test failed, a Mann-Whitney nonparametric test was performed.

Online supplemental material. Table S1 lists the different primers used in the study. Table S2 lists the different antibodies used in the study for Western Blot analysis. Table S3 lists the different antibodies used in the study for flow cytometric analysis. Table S4 describes the number of reads obtained by RNA sequencing for the data presented in Fig. 6. Table S5 describes the location of the primers used by CHIP PCR to locate the putative binding of Irf4 in the promoter of Zbtb20. Online supplemental material is available at http://www.jem.org/cgi/content/full/jem.20131831/DC1.

We are indebted to the facilities of our institute responsible for animal husbandry and flow cytometry. We acknowledge expert technical and statistical assistance from Kathy D'Costa and Yifang Hu, respectively. We are grateful for reagents provided by Drs. Sebastian Carotta, Victor Peperzak, Gabrielle Belz, Axel Kallies, and Ross Dickins and for helpful discussions with Drs. Steve Nutt, Michael Chopin, Frederick Masson, Peter Hickey, and others in B Cell Program at the Walter and Eliza Hall Institute for Medical Research. We are very grateful to Drs. M. Busslinger, M. Minnich, and R. Tooze for generously sharing their unpublished data with us.

This work was supported by the National Health and Medical Research Council (NHMRC) Australia (NHMRC IRIISS grant #361646 and Program grant #575500). S. Chevrier is supported by the Swiss National Science Foundation and W. Shi is supported, in part, by NHMRC Project grant #1023454. This work was made possible through Victorian State Government Operational Infrastructure Support and Australian Government NHMRC IRIIS.

The authors have no conflicting financial interests.

Submitted: 2 September 2013
Accepted: 10 March 2014

REFERENCES

Bahnson, A.B., J.T. Dunigan, B.E. Baysal, T. Mohney, R.W. Atchison, M.T. Nimgaonkar, E.D. Ball, and J.A. Barranger. 1995. Centrifugal enhancement of retroviral mediated gene transfer. *J. Virol. Methods*. 54:131–143. http://dx.doi.org/10.1016/0166-0934(95)00035-S

Beaulieu, A.M., and D.B. Sant'Angelo. 2011. The BTB-ZF family of transcription factors: key regulators of lineage commitment and effector function development in the immune system. *J. Immunol.* 187:2841–2847. http://dx.doi.org/10.4049/jimmunol.1004006

Chevrier, S., and L.M. Corcoran. 2014. BTB-ZF transcription factors, a growing family of regulators of early and late B-cell development. *Immunol. Cell Biol.* doi: 10.1038/icb.2014.20.

Cobaleda, C., A. Schebesta, A. Delogu, and M. Busslinger. 2007. Pax5: the guardian of B cell identity and function. *Nat. Immunol.* 8:463–470. http://dx.doi.org/10.1038/ni1454

Costoya, J.A. 2007. Functional analysis of the role of POK transcriptional repressors. *Brief. Funct. Genomics Proteomics*. 6:8–18. http://dx.doi.org/10.1093/bfgp/elm002

De Silva, N.S., G. Simonetti, N. Heise, and U. Klein. 2012. The diverse roles of IRF4 in late germinal center B-cell differentiation. *Immunol. Rev.* 247:73–92. http://dx.doi.org/10.1111/j.1600-065X.2012.01113.x

Duy, C., J.J. Yu, R. Nahar, S. Swaminathan, S.M. Kweon, J.M. Polo, E. Valls, L. Klemm, S. Shojaee, L. Cerchietti, et al. 2010. BCL6 is critical for the development of a diverse primary B cell repertoire. *J. Exp. Med.* 207:1209–1221. http://dx.doi.org/10.1084/jem.20091299

Emslie, D., K. D'Costa, J. Hasbold, D. Metcalf, K. Takatsu, P.O. Hodgkin, and L.M. Corcoran. 2008. Oct2 enhances antibody-secreting cell differentiation through regulation of IL-5 receptor α chain expression on activated B cells. *J. Exp. Med.* 205:409–421. http://dx.doi.org/10.1084/jem.20072049

Fairfax, K.A., L.M. Corcoran, C. Pridans, N.D. Huntington, A. Kallies, S.L. Nutt, and D.M. Tarlinton. 2007. Different kinetics of blimp-1 induction in B cell subsets revealed by reporter gene. *J. Immunol.* 178:4104–4111.

Fukuda, T., T. Yoshida, S. Okada, M. Hatano, T. Miki, K. Ishibashi, S. Okabe, H. Koseki, S. Hirosawa, M. Taniguchi, et al. 1997. Disruption of the *Bcl6* gene results in an impaired germinal center formation. *J. Exp. Med.* 186:439–448. http://dx.doi.org/10.1084/jem.186.3.439

Gentleman, R.C., V.J. Carey, D.M. Bates, B. Bolstad, M. Dettling, S. Dudoit, B. Ellis, L. Gautier, Y. Ge, J. Gentry, et al. 2004. Bioconductor: open software development for computational biology and bioinformatics. *Genome Biol.* 5:R80. http://dx.doi.org/10.1186/gb-2004-5-10-r80

Humbert, P.O., and L.M. Corcoran. 1997. oct-2 gene disruption eliminates the peritoneal B-1 lymphocyte lineage and attenuates B-2 cell maturation and function. *J. Immunol.* 159:5273–5284.

Jeon, B.N., W.I. Choi, M.Y. Yu, A.R. Yoon, M.H. Kim, C.O. Yun, and M.W. Hur. 2009. ZBTB2, a novel master regulator of the p53 pathway. *J. Biol. Chem.* 284:17935–17946. http://dx.doi.org/10.1074/jbc.M809559200

Kallies, A., J. Hasbold, D.M. Tarlinton, W. Dietrich, L.M. Corcoran, P.D. Hodgkin, and S.L. Nutt. 2004. Plasma cell ontogeny defined by quantitative changes in blimp-1 expression. *J. Exp. Med.* 200:967–977. http://dx.doi.org/10.1084/jem.20040973

Kallies, A., J. Hasbold, K. Fairfax, C. Pridans, D. Emslie, B.S. McKenzie, A.M. Lew, L.M. Corcoran, P.D. Hodgkin, D.M. Tarlinton, and S.L. Nutt. 2007. Initiation of plasma-cell differentiation is independent of the transcription factor Blimp-1. *Immunity.* 26:555–566. http://dx.doi.org/10.1016/j.immuni.2007.04.007

Kelly, K.F., and J.M. Daniel. 2006. POZ for effect—POZ-ZF transcription factors in cancer and development. *Trends Cell Biol.* 16:578–587. http://dx.doi.org/10.1016/j.tcb.2006.09.003

Klein, U., and R. Dalla-Favera. 2007. Unexpected steps in plasma-cell differentiation. *Immunity.* 26:543–544. http://dx.doi.org/10.1016/j.immuni.2007.05.005

Klein, U., S. Casola, G. Cattoretti, Q. Shen, M. Lia, T. Mo, T. Ludwig, K. Rajewsky, and R. Dalla-Favera. 2006. Transcription factor IRF4 controls plasma cell differentiation and class-switch recombination. *Nat. Immunol.* 7:773–782. http://dx.doi.org/10.1038/ni1357

Kosan, C., I. Saba, M. Godmann, S. Herold, B. Herkert, M. Eilers, and T. Möröy. 2010. Transcription factor miz-1 is required to regulate interleukin-7 receptor signaling at early commitment stages of B cell differentiation. *Immunity.* 33:917–928. http://dx.doi.org/10.1016/j.immuni.2010.11.028

Liao, Y., G.K. Smyth, and W. Shi. 2013. The Subread aligner: fast, accurate and scalable read mapping by seed-and-vote. *Nucleic Acids Res.* 41:e108. http://dx.doi.org/10.1093/nar/gkt214

Lin, Y., K. Wong, and K. Calame. 1997. Repression of c-myc transcription by Blimp-1, an inducer of terminal B cell differentiation. *Science.* 276:596–599. http://dx.doi.org/10.1126/science.276.5312.596

Lin, L., A.J. Gerth, and S.L. Peng. 2004. Active inhibition of plasma cell development in resting B cells by microphthalmia-associated transcription factor. *J. Exp. Med.* 200:115–122. http://dx.doi.org/10.1084/jem.20040612

MacLennan, I.C., K.M. Toellner, A.F. Cunningham, K. Serre, D.M. Sze, E. Zúñiga, M.C. Cook, and C.G. Vinuesa. 2003. Extrafollicular antibody responses. *Immunol. Rev.* 194:8–18. http://dx.doi.org/10.1034/j.1600-065X.2003.00058.x

Maeda, T., T. Merghoub, R.M. Hobbs, L. Dong, M. Maeda, J. Zakrzewski, M.R. van den Brink, A. Zelent, H. Shigematsu, K. Akashi, et al. 2007. Regulation of B versus T lymphoid lineage fate decision by the proto-oncogene LRF. *Science.* 316:860–866. http://dx.doi.org/10.1126/science.1140881

Manz, R.A., A.E. Hauser, F. Hiepe, and A. Radbruch. 2005. Maintenance of serum antibody levels. *Annu. Rev. Immunol.* 23:367–386. http://dx.doi.org/10.1146/annurev.immunol.23.021704.115723

McHeyzer-Williams, M., S. Okitsu, N. Wang, and L. McHeyzer-Williams. 2012. Molecular programming of B cell memory. *Nat. Rev. Immunol.* 12:24–34.

Mirman, D., J.A. Dixon, and J.S. Magnuson. 2008. Statistical and computational models of the visual world paradigm: Growth curves and individual differences. *J. Mem. Lang.* 59:475–494. http://dx.doi.org/10.1016/j.jml.2007.11.006

Mitchelmore, C., K.M. Kjaerulff, H.C. Pedersen, J.V. Nielsen, T.E. Rasmussen, M.F. Fisker, B. Finsen, K.M. Pedersen, and N.A. Jensen. 2002. Characterization of two novel nuclear BTB/POZ domain zinc finger isoforms. Association with differentiation of hippocampal neurons, cerebellar granule cells, and macroglia. *J. Biol. Chem.* 277:7598–7609. http://dx.doi.org/10.1074/jbc.M110023200

Mittrücker, H.W., T. Matsuyama, A. Grossman, T.M. Kündig, J. Potter, A. Shahinian, A. Wakeham, B. Patterson, P.S. Ohashi, and T.W. Mak. 1997. Requirement for the transcription factor LSIRF/IRF4 for mature B and T lymphocyte function. *Science.* 275:540–543. http://dx.doi.org/10.1126/science.275.5299.540

Müller, M.M., E. Schreiber, W. Schaffner, and P. Matthias. 1989. Rapid test for in vivo stability and DNA binding of mutated octamer binding proteins with 'mini-extracts' prepared from transfected cells. *Nucleic Acids Res.* 17:6420. http://dx.doi.org/10.1093/nar/17.15.6420

Muto, A., K. Ochiai, Y. Kimura, A. Itoh-Nakadai, K.L. Calame, D. Ikebe, S. Tashiro, and K. Igarashi. 2010. Bach2 represses plasma cell gene regulatory network in B cells to promote antibody class switch. *EMBO J.* 29:4048–4061. http://dx.doi.org/10.1038/emboj.2010.257

Nicol, J.W., G.A. Helt, S.G. Blanchard Jr., A. Raja, and A.E. Loraine. 2009. The Integrated Genome Browser: free software for distribution and exploration of genome-scale datasets. *Bioinformatics.* 25:2730–2731. http://dx.doi.org/10.1093/bioinformatics/btp472

Nielsen, J.V., F.H. Nielsen, R. Ismail, J. Noraberg, and N.A. Jensen. 2007. Hippocampus-like corticoneurogenesis induced by two isoforms of the BTB-zinc finger gene Zbtb20 in mice. *Development.* 134:1133–1140. http://dx.doi.org/10.1242/dev.000265

O'Connor, B.P., V.S. Raman, L.D. Erickson, W.J. Cook, L.K. Weaver, C. Ahonen, L.L. Lin, G.T. Mantchev, R.J. Bram, and R.J. Noelle. 2004. BCMA is essential for the survival of long-lived bone marrow plasma cells. *J. Exp. Med.* 199:91–98. http://dx.doi.org/10.1084/jem.20031330

Ochiai, K., M. Maienschein-Cline, G. Simonetti, J. Chen, R. Rosenthal, R. Brink, A.S. Chong, U. Klein, A.R. Dinner, H. Singh, and R. Sciammas. 2013. Transcriptional regulation of germinal center B and plasma cell fates by dynamical control of IRF4. *Immunity.* 38:918–929. http://dx.doi.org/10.1016/j.immuni.2013.04.009

Oracki, S.A., J.A. Walker, M.L. Hibbs, L.M. Corcoran, and D.M. Tarlinton. 2010. Plasma cell development and survival. *Immunol. Rev.* 237:140–159. http://dx.doi.org/10.1111/j.1600-065X.2010.00940.x

Peperzak, V., I. Vikström, J. Walker, S.P. Glaser, M. LePage, C.M. Coquery, L.D. Erickson, K. Fairfax, F. Mackay, A. Strasser, et al. 2013. Mcl-1 is essential for the survival of plasma cells. *Nat. Immunol.* 14:290–297. http://dx.doi.org/10.1038/ni.2527

Peterson, M.L., C. Ma, and B.T. Spear. 2011. Zhx2 and Zbtb20: novel regulators of postnatal alpha-fetoprotein repression and their potential role in gene reactivation during liver cancer. *Semin. Cancer Biol.* 21:21–27.

Phan, R.T., M. Saito, K. Basso, H. Niu, and R. Dalla-Favera. 2005. BCL6 interacts with the transcription factor Miz-1 to suppress the cyclin-dependent kinase inhibitor p21 and cell cycle arrest in germinal center B cells. *Nat. Immunol.* 6:1054–1060. http://dx.doi.org/10.1038/ni1245

Revilla-I-Domingo, R., I. Bilic, B. Vilagos, H. Tagoh, A. Ebert, I.M. Tamir, L. Smeenk, J. Trupke, A. Sommer, M. Jaritz, and M. Busslinger. 2012. The B-cell identity factor Pax5 regulates distinct transcriptional programmes in early and late B lymphopoiesis. *EMBO J.* 31:3130–3146.

Rosenthal, E.H., A.B. Tonchev, A. Stoykova, and K. Chowdhury. 2012. Regulation of archicortical arealization by the transcription factor Zbtb20. *Hippocampus.* 22:2144–2156.

Saito, M., U. Novak, E. Piovan, K. Basso, P. Sumazin, C. Schneider, M. Crespo, Q. Shen, G. Bhagat, A. Califano, et al. 2009. BCL6 suppression of BCL2 via Miz1 and its disruption in diffuse large B cell lymphoma. *Proc. Natl. Acad. Sci. USA.* 106:11294–11299. http://dx.doi.org/10.1073/pnas.0903854106

Sakurai, N., M. Maeda, S.U. Lee, Y. Ishikawa, M. Li, J.C. Williams, L. Wang, L. Su, M. Suzuki, T.I. Saito, et al. 2011. The LRF transcription factor regulates mature B cell development and the germinal center response in mice. *J. Clin. Invest.* 121:2583–2598. http://dx.doi.org/10.1172/JCI45682

Samardzic, T., D. Marinkovic, P.J. Nielsen, L. Nitschke, and T. Wirth. 2002. BOB.1/OBF.1 deficiency affects marginal-zone B-cell compartment. *Mol. Cell. Biol.* 22:8320–8331. http://dx.doi.org/10.1128/MCB.22.23.8320-8331.2002

Sciammas, R., A.L. Shaffer, J.H. Schatz, H. Zhao, L.M. Staudt, and H. Singh. 2006. Graded expression of interferon regulatory factor-4 coordinates isotype switching with plasma cell differentiation. *Immunity*. 25:225–236. http://dx.doi.org/10.1016/j.immuni.2006.07.009

Shaffer, A.L., K.I. Lin, T.C. Kuo, X. Yu, E.M. Hurt, A. Rosenwald, J.M. Giltnane, L. Yang, H. Zhao, K. Calame, and L.M. Staudt. 2002. Blimp-1 orchestrates plasma cell differentiation by extinguishing the mature B cell gene expression program. *Immunity*. 17:51–62. http://dx.doi.org/10.1016/S1074-7613(02)00335-7

Shaffer, A.L., M. Shapiro-Shelef, N.N. Iwakoshi, A.H. Lee, S.B. Qian, H. Zhao, X. Yu, L. Yang, B.K. Tan, A. Rosenwald, et al. 2004. XBP1, downstream of Blimp-1, expands the secretory apparatus and other organelles, and increases protein synthesis in plasma cell differentiation. *Immunity*. 21:81–93. http://dx.doi.org/10.1016/j.immuni.2004.06.010

Shapiro-Shelef, M., K.I. Lin, L.J. McHeyzer-Williams, J. Liao, M.G. McHeyzer-Williams, and K. Calame. 2003. Blimp-1 is required for the formation of immunoglobulin secreting plasma cells and pre-plasma memory B cells. *Immunity*. 19:607–620. http://dx.doi.org/10.1016/S1074-7613(03)00267-X

Shi, W., A. Oshlack, and G.K. Smyth. 2010. Optimizing the noise versus bias trade-off for Illumina whole genome expression BeadChips. *Nucleic Acids Res*. 38:e204. http://dx.doi.org/10.1093/nar/gkq871

Smyth, G.K. 2004. Linear models and empirical bayes methods for assessing differential expression in microarray experiments. *Stat. Appl. Genet. Mol. Biol*. 3:e3.

Sutherland, A.P., H. Zhang, Y. Zhang, M. Michaud, Z. Xie, M.E. Patti, M.J. Grusby, and W.J. Zhang. 2009. Zinc finger protein Zbtb20 is essential for postnatal survival and glucose homeostasis. *Mol. Cell. Biol*. 29:2804–2815. http://dx.doi.org/10.1128/MCB.01667-08

Taubenheim, N., D.M. Tarlinton, S. Crawford, L.M. Corcoran, P.D. Hodgkin, and S.L. Nutt. 2012. High rate of antibody secretion is not integral to plasma cell differentiation as revealed by XBP-1 deficiency. *J. Immunol*. 189:3328–3338. http://dx.doi.org/10.4049/jimmunol.1201042

Tunyaplin, C., A.L. Shaffer, C.D. Angelin-Duclos, X. Yu, L.M. Staudt, and K.L. Calame. 2004. Direct repression of prdm1 by Bcl-6 inhibits plasmacytic differentiation. *J. Immunol*. 173:1158–1165.

Turner, C.A. Jr., D.H. Mack, and M.M. Davis. 1994. Blimp-1, a novel zinc finger-containing protein that can drive the maturation of B lymphocytes into immunoglobulin-secreting cells. *Cell*. 77:297–306. http://dx.doi.org/10.1016/0092-8674(94)90321-2

Victora, G.D., and M.C. Nussenzweig. 2012. Germinal centers. *Annu. Rev. Immunol*. 30:429–457. http://dx.doi.org/10.1146/annurev-immunol-020711-075032

Weber, A., J. Marquardt, D. Elzi, N. Forster, S. Starke, A. Glaum, D. Yamada, P.A. Defossez, J. Delrow, R.N. Eisenman, et al. 2008. Zbtb4 represses transcription of P21CIP1 and controls the cellular response to p53 activation. *EMBO J*. 27:1563–1574. http://dx.doi.org/10.1038/emboj.2008.85

Xie, Z., H. Zhang, W. Tsai, Y. Zhang, Y. Du, J. Zhong, C. Szpirer, M. Zhu, X. Cao, M.C. Barton, et al. 2008. Zinc finger protein ZBTB20 is a key repressor of alpha-fetoprotein gene transcription in liver. *Proc. Natl. Acad. Sci. USA*. 105:10859–10864. http://dx.doi.org/10.1073/pnas.0800647105

Yoon, H.S., C.D. Scharer, P. Majumder, C.W. Davis, R. Butler, W. Zinzow-Kramer, I. Skountzou, D.G. Koutsonanos, R. Ahmed, and J.M. Boss. 2012. ZBTB32 is an early repressor of the CIITA and MHC class II gene expression during B cell differentiation to plasma cells. *J. Immunol*. 189:2393–2403.

Zhang, W., J. Mi, N. Li, L. Sui, T. Wan, J. Zhang, T. Chen, and X. Cao. 2001. Identification and characterization of DPZF, a novel human BTB/POZ zinc finger protein sharing homology to BCL-6. *Biochem. Biophys. Res. Commun*. 282:1067–1073. http://dx.doi.org/10.1006/bbrc.2001.4689

Zotos, D., J.M. Coquet, Y. Zhang, A. Light, K. D'Costa, A. Kallies, L.M. Corcoran, D.I. Godfrey, K.M. Toellner, M.J. Smyth, et al. 2010. IL-21 regulates germinal center B cell differentiation and proliferation through a B cell–intrinsic mechanism. *J. Exp. Med*. 207:365–378. http://dx.doi.org/10.1084/jem.20091777